

Airflow and insulation effects on simultaneous syngas and biochar production in a top-lit updraft biomass gasifier

Arthur M. James R.^{a,b}, Wenqiao Yuan^{a,*}, Michael D. Boyette^a, Donghai Wang^c

^a Department of Biological and Agricultural Engineering, North Carolina State University,
Campus Box 7625, Raleigh, NC 27695 USA

^b Department of Mechanical Engineering, Universidad Tecnologica de Panama, Apartado
0819-07289, El Dorado, Panama

^c Department of Biological and Agricultural Engineering, Kansas State University, 129
Seaton Hall, Manhattan, KS 66506 USA

*corresponding author. Tel.: +1 9195156742; fax: +1 9195157760; email:

w yuan2@ncsu.edu

Abstract

The objective of this study was to understand the effect of airflow and insulation on syngas and biochar generations of rice hulls and woodchips in a top-lit updraft gasifier. Biochar yield decreased with increasing airflow. The highest biochar yields of 39% and 27% were achieved at 8 L/min airflow for rice hulls and woodchips, respectively. The mass fraction of syngas in the products increased with increasing airflow, which ranged from 88 to 89% for rice hulls and 93 to 94% for woodchips. The H₂ composition in syngas also increased at higher airflow rates; it peaked at 4.2-4.4% for rice hulls and 5.7-6.6% (v/v) for woodchips, which was not affected by insulation. The carbon monoxide content in syngas ranged from approximately 12 to 15% (v/v) and was not affected by airflow or insulation. Average tar content in syngas decreased for both biomasses when airflow increased, but

adding insulation resulted in significantly higher tar content in syngas. The biomass type also had significant effects on gasifier performance. Biochar yields from rice hulls were greater than that from woodchips at all airflow rates. The lowest tar contents in syngas were approximately 1.16 and 11.88 g/m³ for rice hulls and woodchips, respectively.

Keywords: gasification; top-lit updraft; biochar; tar; syngas.

1. Introduction

Utilization of renewable biomass resources to generate bioenergy and bio-products has increased significantly in the last decades (Casler et al., 2009; McCord et al., 2014). Among various technological choices, biomass gasification is relatively simple in process/reactor design and implementation (Hasan et al., 2010). It generally produces two potentially useful products: syngas and biochar. Syngas contains hydrogen and carbon monoxide that can be used to fuel internal combustion engines, turbines and boilers (Knoef, 2005); it can also be used to produce a wide variety of fuels and chemicals, such as gasoline, diesel and α -olefins via the Fischer-Tropsch process (Dry, 2002), ethanol by biological conversion or catalytic reactions, or ammonia and methanol via catalytic hydrogenation (Jadhav et al., 2014; Griffin and Schultz, 2012). Biochar is known for its carbon-rich nature that provides valuable benefits to the environment (Lorenz and Lal, 2014). It can be used in a broad number of applications such as removal of pollutants in aqueous and gas media, and as a soil conditioner to improve plant growth (Hyland and Sarmah, 2014; Joseph et al., 2009).

However, common methods for biochar production are reported to have high energy input and/or severe emissions of contaminants (Garcia-Perez et al., 2010). For instance, kilns and retorts in developing countries are known to release carbon monoxide, non-methane volatiles and particulate matters to the environment (Sparrevik et al., 2015). Modified pyrolysis units have been reported to reduce pollutant emissions and increase the yield of biochar (Brown, 2009). For example high-pressure pyrolysis reactors can produce biochar from 41 to 62% yields with minimal emissions; however, the use of high pressures (0.4 to 1 MPa) represents a major disadvantage (Antal et al., 1996). Another example is the multistage pyrolysis reactors in which the progressive increase in reaction temperature reduced the energy input by 30% and achieved biochar yield of up to 27% (Oyedun et al., 2012). However, these technologies require higher energy input compared to gasification systems. Common gasification processes such as downdraft gasifiers and fluidized-bed gasifiers are aimed for the production of syngas only (Knoef, 2005). On the other hand, top-lit updraft (TLUD) gasification has the potential for simultaneous production of biochar and syngas from biomass. Some variations of TLUD gasifiers have been found to produce relatively high yields of biochar and parallel production of syngas (Birzer et al., 2013; Tryner et al., 2014). The syngas generated in top-lit updraft gasifiers can be combusted to increase the energy efficiency of biochar production (Knoef, 2005). However, previous studies were mostly focused on the utilization of TLUD gasifiers to fuel cookstoves in developing countries (Panwar and Rathore, 2008). There is not a full understanding of the process from the perspective of how gasification-medium flow rate (e.g. air), biomass type, and gasifier design affect simultaneous syngas and biochar production (Lehmann and Joseph, 2009).

The objective of this work was to understand the effect of varying biomass type, air flow rate and reactor insulation on TLUD gasification through the quantification of biochar, syngas and tar products. Two biomasses (rice hulls and woodchips) were studied at four airflow rates. For each condition, the TLUD gasifier was operated with and without insulation on its external surface.

2. Materials and methods

2.1 The gasification unit and tar and syngas sampling systems

The gasification unit consisted of a 152 cm high black iron tube with 10.1 cm diameter (Fig. 1). Air was supplied to the reactor with an air compressor (1.5 kW – 8.62 bar maximum operational pressure) equipped with an 18.92 liter reservoir tank (WEN, Elgin, IL). A perforated plate with 3 mm diameter holes made of commercial galvanized steel was placed 10 cm from the bottom of the gasifier to provide a uniform air distribution within the reactor. The gasifier inlet air was maintained at 2.1 bar with a pressure regulator, and the airflow rate was adjusted using a variable area flow meter (Cole-Parmer 150-mm, max. pressure 13.8 bar, Chicago, IL). The outlet was open to the atmosphere. The temperatures at the top, middle and bottom of the gasifier were measured by type-K thermocouples and recorded with a data logger (Measurement Computing, model: USB-5201, Norton, MA). Tar in the syngas was collected 15 min after the reaction started. This procedure was performed using a two-stage cold trapping method (James et al., 2016a); the first stage contained two flasks cooled by ice (0°C) in which heavy tars and water were collected. In the second stage, two flasks under dry ice (solid carbon dioxide) cooled the syngas and condensed the remaining tars in the gas. When sampling tars, half of the intake airflow for gasification was used (e.g., when airflow rate was 8 L/min (lpm) the tar

sampling flow was set at 4 lpm) for 45 min. The tar samples were evaporated for 24 hours at 105°C; the final weight of the dry material was defined as tar. Tar in biochar was determined by solvent extraction. One gram of biochar was placed in 25 ml of acetone and agitated for 4 hours. After that, the solid was washed with 25 ml of acetone again, then they were filtered with a 110-mm diameter filter paper (Whatman™ Qualitative #1) to remove biochar. The biochar was dried at 105°C for 1 hour to measure its dry weight. The weight difference between the initial biochar and the washed biochar was used to determine the percentage of weight loss and reported as tar in biochar. Syngas samples were collected in 0.5 liter Tedlar® sampling bags and analyzed in a gas chromatography (SRI8610C, Torrance, CA) equipped with a thermal conductivity detector using helium as the carrier gas. Compositions of H₂, CO, CO₂, CH₄, O₂ and N₂ were determined.

Fig.1

2.2 Experimental procedures

Gasification was evaluated at 4 levels of airflow rate (8, 12, 16 and 20 lpm) and two insulation conditions (no insulation or insulating the reactor with 88.9 mm Pinkplus Fiberglass® on the external wall). The equivalent superficial velocities for the four airflow rates were 0.83, 1.25, 1.66 and 2.08 cm/s, respectively. Rice hulls from Carolina Greenhouses (Kinston, NC) and pine woodchips from a local grinding company (Newton County, NC) were used as the feedstocks. The particle size of the rice hulls was measured using different screen sizes and the average particles were smaller than 2 mm. Pine woodchips had particle sizes smaller than 10 mm. Particles smaller than 3 mm were removed using a 3-mm screen, thus the final particle size of the woodchips ranged

between 3 and 10 mm. The two biomasses had noticeable differences in chemical composition and their major properties are presented in Table 1. The carbon and volatile matter contents of woodchips were approximately 10% and 16% points higher, respectively, compared to rice hulls, whereas the ash content in rice hulls was ~23% points higher than woodchips.

The operating procedure of the gasifier was as follows. Once the gasifier was loaded, the top layer of biomass in the gasifier was lit with a propane torch for 1 min; this initial heat supplied the needed energy for the pyrolysis reactions to start. Thereafter, air was injected from the bottom and the pyrolysis front started moving downward leaving biochar on the top and producing syngas. Once the peak reaction temperature was sensed by the bottom thermocouple, the reaction was complete and stopped. Then, biochar was collected and the yield of biochar was calculated based on the dry weight of biomass and the final dried biochar weight using the following equation: Biochar yield (wt.%) = $BC / BM \times 100$, where BC is the dry weight of biochar in grams and BM is the dry weight of biomass in grams. Statistical analysis of the results was performed using SAS® software. The GLM procedure was used for multiple comparisons of the flow rates and insulation cases. Tukey HSD method was used for significance analysis ($\alpha=0.1$).

Table 1

3. Results and discussion

3.1 The temperature profiles of the gasifier

Reaction temperature was found to correlate with airflow rate. Increase in airflow resulted in increased pyrolysis front temperature (PFT) for the two biomasses at the two

insulation conditions, as shown in Fig. 2A and 2B. The pyrolysis front temperature was defined as the average peak temperature measured by the four thermocouples once the pyrolysis front reached the thermocouples. The PFT of rice hulls consistently increased from 700 to 862°C without insulation ($R^2=0.99$), and from 714 to 868°C ($R^2=0.98$) with insulation. Similarly, the PFT of woodchips increased from 648 to 815°C ($R^2=0.95$) without insulation and from 661 to 840°C ($R^2=0.96$) with insulation. This increase in the PFT complied with previous findings that the temperature of thermochemical reactions was strongly influenced by the amount of air provided to the combustion of the system; increase in air supply for gasification was found to increase the reaction temperature (Ma et al., 2015).

From Fig. 2, it can be seen that gasification of rice hulls presented slightly higher PFT's than woodchips. The Stoichiometric air to fuel ratios for rice hulls and woodchips were 3.63 and 3.94, respectively, which implied that when the same amount of air was provided to rice hulls, one could expect to see higher reaction temperature than woodchips due to more available air (Weiland et al., 2015). The air-fuel equivalence ratios for all experiments in this study were reported in a previous paper (James et al., 2016b). Rice hulls had higher air-fuel equivalence ratios than woodchips at the same setting. The linear correlation between the pyrolysis front temperature and the equivalence ratio for rice hulls and woodchips had average R^2 of 0.94 and 0.93, respectively. Previous work by other researchers (Ma et al., 2015; Lv et al. 2007) also showed similar correlations between PFT and air-fuel equivalence ratio.

The addition of insulation seemed to increase the PFT. However, the statistical comparison of the PFT for individual biomasses at every airflow rate presented no significant differences in the PFT when insulation was added. In order to evaluate the

effect of insulation on the reaction temperature, the average reaction temperature (ART) was calculated. The ART was defined as the 40 min average temperature after the pyrolysis front passed thermocouple #1 (TC-1). In other words, once thermocouple #1 reached its peak temperature (the pyrolysis front temperature), the timing started and all temperatures were recorded for forty minutes, and the average of all temperatures in the 40-min period was used as the average reaction temperature. In contrast, Peterson et al. (2014) called “average temperature” the average peak temperature of individual thermocouples, which was the pyrolysis front temperature in this work. Thus, our average reaction temperature was different from pyrolysis front temperature. The ART could help us understand how fast the temperature decreased within the gasifier at different airflows and insulation conditions. It can be seen from Fig. 2C and 2D that no insulation resulted in lower average reaction temperatures which were not significantly different between the two biomasses at every airflow rate. However, the utilization of insulation exhibited linear increase with the airflow rate for both biomasses ($R^2=0.98$). This suggests that the insulation on the reactor considerably helped to reduce heat loss through the gasifier’s wall; as a result, higher average temperatures of the biomass bed were achieved after the pyrolysis front had passed.

Fig. 2

Fig. 3A and 3B show the temperature profiles of the two biomasses and two insulation conditions using 12 lpm as an example. It can be seen that once the flame reached the first thermocouple (TC-1), the temperature rapidly increased from the ambient temperature to the peak temperature. This sudden increase of temperature as the

pyrolysis front moved had been previously reported when a top-lit updraft cookstove was tested. The authors found that the temperature of the biomass abruptly increased from the ambient temperature to ~600°C when wheat straw was gasified (Peterson and Jackson, 2014). Differences in the pace of cooling can also be observed when comparing the temperature profiles of insulation and no insulation. The insulated gasifier cooled slower, and the pyrolysis front reached the next thermocouple sooner because of the improved heat distribution.

Fig. 3

3.2 The burning rate of biomass

The burning rate was defined as the speed at which the flame traveled from the top to the bottom of the gasifier (mm/min). It was calculated using the time elapse that the flame (the highest temperature) reached the top (TC-1) and middle (TC-2) thermocouples as presented in Fig. 3A and 3B. In Fig. 3C and 3D, the burning rates of rice hulls and woodchips are presented at the varying airflows and the two insulation cases. When rice hulls were gasified, increase in the airflow rate from 8 to 20 lpm resulted in increasing burning rates for no insulation and insulation as follows: 11.6 to 18.3 mm/min and 12.6 to 19.1 mm/min, respectively. Similarly, in the gasification of woodchips, it was noticed that the burning rate increased as more air for gasification was supplied. Without insulation, the burning rate varied from 6.3 to 10.2 mm/min and with insulation from 8.1 to 13.2 mm/min when increasing the airflow rate. Burning rate was found to linearly correlate with airflow rate ($R^2 = 0.95 - 0.99$). Ryu et al. (2006) also found a positive linear correlation between the biomass burning rate and the airflow when biomass was oxidized in a fixed

bed reactor. The increase in the burning rate at higher airflow rates was consistent with the increase in PFT because more fuel (biomass) was needed to promote the generation of heat in combustion reactions. Despite the fact that PFT did not significantly increase at different insulation conditions, the insulation increased the overall reaction temperature (Fig. 2). As a result, the burning rate further increased because more heat that was initially lost through the gasifier walls was now used to devolatilize the biomass in the gasifier chamber.

3.3 The yield of biochar

Biochar yield of the two biomasses decreased as the airflow rate increased (Fig. 4A and 4B). When airflow increased from 8 to 20 lpm, the yield of biochar from rice hulls reduced from 38.0 to 31.6% and from 39.3 to 31.3% for no insulation and with insulation, respectively. Lower biochar yields were observed in the gasification of woodchips than rice hulls. Without insulation, the biochar yield was reduced from 27.1 to 12.9% and with insulation from 18.8 to 12.3%. This decrease in biochar yield with increasing airflow can be correlated with the progressive increase in PFT ($R^2=0.93$). Most of the fuel for the combustion reactions in top-lit updraft gasifier is provided by the volatiles released during the pyrolysis of the immediate biomass below the pyrolysis front (Saravanakumar et al., 2007); however, the increase in the airflow can also promote the combustion of the biochar layer that was formed above the combustion flame. A well-known representation of this process can be observed in a flaming match where the pyrolysis vapors from the internal reactions of the wood were released fueling the flame and producing biochar (Tryner et al., 2016). In another previous work, Demirbas (2001) reported that the biochar yield decreased with increasing carbonization temperature, which was consistent with Fig.

4A and 4B when compared with Fig. 2. From Fig. 4A, it can also be observed that there were no significant differences in the yield of biochar from rice hulls between insulation and no insulation. Moreover, the yield of biochar from woodchips showed different behaviors than that presented by rice hulls at lower airflow rates. The addition of insulation considerably reduced the yield of biochar at 8 lpm (18.8% yield) and 12 lpm (16.2% yield).

Fig. 4

Fig. 4C and 4D present the percentages of tar in biochar from rice hulls and woodchips. The configuration of the TLUD gasifier promotes the retention of condensable tar in the biochar. This is because the syngas flows within the biochar carrying pyrolysis products. Rice hull biochar generated from the insulated reactor showed tar contents ranging from 0.63 to 0.84 wt. %. Without insulation the tar content in biochar was generally higher, reaching 2.29 wt. % at 12 lpm (Fig. 4C). Tar in biochar from woodchips had similar trends as presented in Fig. 4D. Large amounts of tar were found in the biochar when no insulation was used, which however decreased from 14.9 to 0 wt. % as the airflow increased from 8 to 20 lpm. With the use of insulation, the highest tar content in woodchip biochar was only 0.07 wt. % at 8 lpm and no tar was found at higher airflow rates. Overall, the biochar produced from the insulated gasifier contained less than 1 wt. % tars, in the same way, less tar was found at higher airflow rates regardless of the insulation condition. Biochar with low tar content can be directly used for certain applications such as to make activated carbon and soil conditioner (Manya, 2012; Downie et al., 2009) in which the tar content might be a concern. Consideration between tar in biochar and tar in syngas needs to be taken into account when selecting a specific airflow

rate and gasifier configuration. Biochar with excessive tar might require further treatments after production; this can increase the operational cost of biochar production.

3.4 Syngas compositions

Table 2 shows the composition of hydrogen in syngas from rice hulls and woodchips at different airflow rates and insulation conditions. H₂ content generally increased when the airflow increased. For example, rice hull syngas contained 2.3 to 4.2 vol. % and 2.8 to 4.4 vol. % H₂, for no insulation and with insulation conditions, respectively. In a similar way, when airflow increased from 8 to 20 lpm, the hydrogen content in syngas from woodchips increased from 2.5 to 5.7 vol. % and from 3.3 to 6.6 vol. % for without insulation and with insulation conditions, respectively. Hydrogen content in syngas was positively correlated with PFT ($R^2 = 0.85$). However, insulation had no significant effects on the hydrogen content when independent airflow rates were compared. This increase in the hydrogen content as result of increasing reaction temperature was believed to be due to the oxidation and cracking of tars (Galindo et al., 2014). Lv et al. (2004) reported a similar tendency in hydrogen content that increased from 22 to 40 vol. % when the temperature increased from 700 to 900°C.

Table 2

Table 2 presents CO composition of rice hulls and woodchips at different levels of insulation. As the airflow rate increased from 8 to 20 lpm, little difference was noticed in CO composition of rice hulls (12.3 to 15.8 vol. %). Similarly, the CO composition in syngas from woodchips varied from 11.4 to 14.9 vol. % when increasing the airflow rate. No

significant differences in CO composition at different levels of airflow rates and insulation conditions were observed except for woodchips at 8 lpm without insulation, at which the CO composition was significantly lower (11.45 vol. %). It can be found from Fig. 2 that woodchips at 8 lpm without insulation had very low pyrolysis font temperature (~650 °C), which was close to pyrolysis rather than gasification, thus CO generation was low. Other conditions were closer to gasification with higher temperatures and stable CO generation, similar to those presented by Turn et al. (1998).

3.5 Tar content in syngas

Results of tar content in syngas are presented in Fig. 5. Airflow rate for rice hull gasification without insulation had no significant effects on syngas tar contents. However, the utilization of insulation significantly increased the concentration of tar especially at lower airflow rates. When insulating the reactor, airflow of 8 lpm was found to produce the highest tar content of 16.6 g/m³ for rice hulls, which was reduced to 2.76 g/m³ at 20 lpm (Fig. 5A). Gasification of woodchips showed much higher tar contents, which decreased from 58.7 to 11.8 g/m³ as the airflow rate increased from 8 to 20 lpm without insulation. Insulation also significantly increased tar contents in syngas from woodchips. The highest tar content for woodchips was 86.2 g/m³ at 8 lpm (insulated, Fig. 5B). The decrease in tar content with increasing airflow suggested that raising the combustion temperature can reduce the subsequent production of tar in syngas. Previous gasification studies reported that the generation of tar was discouraged by the increase in the reaction temperature (Milne et al., 1998; Hanping et al., 2008; Demirbas, 2001). Similarly, increasing the airflow also increases the equivalence ratio (ER) at which the biomass reacts. It has been demonstrated that at low ER (close to 0) pyrolysis reactions predominate, increasing the

production of condensable aromatic hydrocarbons including tars; however, at higher ER (close to 1) complete combustion is approached promoting the production of gases (Knoef, 2005) without tars. There were three possible causes for the higher tar contents in syngas from the insulated reactor. In a TLUD gasifier, the heat from incomplete combustion or pyrolysis of the biomass enables charcoaling and tar formation. As a result, the improved heat distribution when the gasifier was insulated tended to increase the production of condensable aromatic hydrocarbons. The configuration of the TLUD gasifier also played a role. As the biomass reacted, the produced biochar was left on the top and the syngas and condensable gases moved upward within the biochar layers. As can be seen from Figure 2, lower airflow or the absence of insulation was associated with lower average temperature across the gasifier, which caused condensation of tar in the biochar (Fig. 4C and 4D). Therefore, the higher tar content in syngas with insulated reactor might partially be the result of the less tar condensation in biochar due to a higher average temperature of reaction in the unit. When tars were not condensed in biochar, they stayed in syngas and were collected as tar in syngas. Another possible reason is that the biomass burned faster when the reactor was insulated. Because tar was collected for the same amount of time (45 min after stable gasification was achieved) no matter the reactor was insulated or not, more biomass was burned and more tars were made in the same duration when the reactor was insulated. However, the increased burning rate alone was not enough to explain the increases in tars by comparing Fig. 3C and 3D to Fig. 5A and 5B, respectively, thus all the three causes abovementioned might co-exist.

Fig. 5

3.6 The effect of biomass type

Table 3 summarizes the statistical analyses with ANOVA multiple comparison procedure between rice hulls and woodchips. The results showed that PFT had similar tendency for both biomasses, but it was significantly higher for rice hulls at the same airflow rate from 8 to 16 lpm. However, at 20 lpm the PFT of the two biomasses were not significantly different. In contrast, no differences were noticed in the average reaction temperature between the two biomasses. The burning rate of rice hulls was higher than that of woodchips at all levels of airflow rate. This could be explained by comparing the particle size and bulk density of the two biomasses. Rice hulls had particles with sizes lower than 2 mm. In contrast, woodchips had particle sizes between 3 and 10 mm. Likewise, rice hulls presented a lower bulk density of 1.27 g/cm³ compared with woodchips of 2.11 g/cm³. The thin configuration of the rice hull particles contributed to faster devolatilization of the biomass and faster burning rate (Hernandez et al., 2010).

Rice hulls had higher biochar yield than woodchips at all airflow rates. High yield along with high ash content of biochar from rice hulls was an indication of the large amount of inorganic components in the source biomass (Antal and Gronli, 2003). Woodchips also resulted in larger amounts of tars than rice hulls. This difference can be associated with the bulk density of the biomass. Because woodchips had approximately two times the bulk density of rice hulls, more mass of woodchips was concentrated in the same volume of reaction area, which consequently resulted in more tars. Similarly, James et al. (2015) compared tar generation from a woody biomass and a low bulk density biomass (sorghum biomass) in an updraft biomass gasifier when varying the ER from 0.21 to 0.29. The results showed that the overall production of tar from sorghum biomass was 3 g/m³ but 8 g/m³ from woodchips at similar gasification conditions. This suggested that the excessive release of volatile components produced by biomass with higher bulk density could be

attributed to the fact that there was more biomass per unit volume. Therefore, more condensable products were generated when compared with low bulk density biomasses.

The hydrogen contents in syngas of woodchips were significantly higher than rice hulls at the same airflow rate from 12 to 20 lpm, however, no differences were found in CO composition or the higher heating value of syngas from the two biomasses at all airflow rates.

Table 3

3.7 The mass balance of the gasification process

Fig. 6A and 6B present the mass fraction of rice hull gasification products per the total input including biomass and air. It can be seen that the increase in airflow rate reduced the amount of biochar produced, but it encouraged the production of gases. Tar in syngas was negligible. This relative increase in the gas phase and decrease in the solid phase (biochar) can be explained by the increase in PFT as a result of increasing airflow for reactions. Demirbas (2001) reported that increase in the reaction temperature reduced the amount of biochar and tar during biomass carbonization. This phenomenon encourages the production of gases when biomass is reacted at higher temperatures. The effect of insulation can also be observed in Fig 6A and 6B. At low airflow rates (e.g., 8 and 12 lpm), the addition of insulation promoted 7-8% points increase in the gas phase. At high airflow rates (e.g., 16 and 20 lpm), the differences were small and not significant.

Gasification of woodchips (Fig. 6C and 6D) presented similar tendency in mass fraction of products to that of rice hulls. As the airflow rate increased the biochar fraction was minimized and the gas phases increased. Gases from gasification increased from 80 to 94%

when the reactor was not insulated, and from 82 to 93% when insulated. The addition of insulation stimulated the generation of tars in the syngas at low airflow rates. For both biomasses, the moisture content of biochar was reduced when the airflow rate increased without insulation. No moisture was found in the biochar when insulation was added, probably because of higher average temperatures in the reactor that evaporated all water in the biomass and biochar.

Common gasification systems designed to maximize syngas production have mass fraction distributions of approximately 10% biochar, 85% gases and 5% liquids (Brick and Lyutse, 2010). It can be observed that these conditions were approached as the airflow rate increased in the top-lit updraft gasifier. This fact can help to select appropriate operational parameters for this reactor when the production of either syngas or biochar is desired.

Fig. 6

The innovation of this work lies in the detailed understanding of product distribution of top-lit updraft gasification. Syngas, biochar and tar were analyzed and presented, and they were correlated with the airflow rate, insulation condition and biomass type. Most previous work has focused on general gasification, but not relevant to top-lit updraft gasification. With rarely found work on top-lit updraft gasification, the focus was mainly on the production of heat or biochar, which left a gap to better understand how the gasification factors affect the overall performance of the gasifier.

4. Conclusions

The airflow rate and addition of insulation on the external wall of the top-lit updraft gasifier significantly influenced gasifier performance. The hydrogen composition in syngas increased with increasing airflow, but biochar yield was reduced. Insulation led to rising biomass burning rate and reduced biochar yield. It also reduced tars in the biochar but tars in syngas increased significantly. The biomass type also played a significant role in the process. Rice hulls showed much higher biochar yield but woodchips generated more tars and hydrogen gas in the syngas. Carbon monoxide composition in syngas was generally not affected by airflow or insulation.

5. Acknowledgements

This material was based upon the work supported by the U.S. Department of Agriculture and Sun Grant (Award No. 2010-38502-21836 and Subaward No. AB-5-67630. KSU11) and the USDA National Institute of Food and Agriculture, Hatch Project NC02613. The lead author was also partially supported by the scholarship program of IFARHU-SENACYT from the Government of Panama. We would also like to thank Mr. Justin Macialek, a research assistant at North Carolina State University, for his help building the top-lit updraft gasifier.

6. References cited

1. Antal, M.J., Croiset, E., Dai, X., DeAlmeida, C., Mok, W.S., Norberg, N., Richard, J., Al Majthoub, M., 1996. High-yield biomass charcoal, *Energy Fuels*. 10, 652-658.
2. Antal, M.J., Grønli, M., 2003. The art, science, and technology of charcoal production, *Ind. Eng. Chem. Res.* 42, 1619-1640.

3. Bejan, A., 2006. Advanced engineering thermodynamics, third ed. John Wiley & Sons, Hoboken, NJ.
4. Birzer, C., Medwell, P., Wilkey, J., West, T., Higgins, M., MacFarlane, G., Read, M., 2013. An analysis of combustion from a top-lit up-draft (TLUD) cookstove, *Journal of Humanitarian Engineering*. 2, 1-7.
5. Brick, S., Lyutse, S., 2010. Biochar: Assessing the promise and risks to guide US policy, Natural Resources Defense Council Issue Paper. Available at: http://www.nrdc.org/energy/files/biochar_paper.pdf (last accessed 3 November 2015).
6. Brown, R., 2009. Biochar production technology, in Lehmann J., Joseph S. (Eds.), *Biochar production technology, Biochar for environmental management: Science and technology*, first ed. Earthscan, London, p.p. 127-146.
7. Casler, M.D., Mitchell, R., Richardson, J., Zalesny, R.S., 2009. Biofuels, bioenergy, and bioproducts from sustainable agricultural and forest crops. *BioEnergy Research*. 2, 77-78.
8. Demirbas, A., 2004. Effects of temperature and particle size on bio-char yield from pyrolysis of agricultural residues. *J. Anal. Appl. Pyrolysis*. 72, 243-248.
9. Demirbas, A., 2001. Carbonization ranking of selected biomass for charcoal, liquid and gaseous products. *Energy Conversion and Management*. 42, 1229-1238.
10. Dry, M.E., 2002. The Fischer–Tropsch process: 1950–2000. *Catalysis Today*. 71, 227-241.
11. Griffin, D.W., Schultz, M.A., 2012. Fuel and chemical products from biomass syngas: a comparison of gas fermentation to thermochemical conversion routes. *Environmental Progress & Sustainable Energy*. 31, 219-224.

12. Hanping, C., Bin, L., Haiping, Y., Guolai, Y., Shihong, Z., 2008. Experimental investigation of biomass gasification in a fluidized bed reactor. *Energy Fuels*. 22, 3493-3498.
13. Hasan, J., Keshwani, D.R., Carter, S.F., Treasure, T.H., 2010. Thermochemical Conversion of Biomass to Power and Fuels. In Cheng J. (Ed.), *Biomass to Renewable Energy Processes*. CRC Press, Boca Raton, pp. 437-489.
14. Hernández, J.J., Aranda-Almansa, G., Bula, A., 2010. Gasification of biomass wastes in an entrained flow gasifier: Effect of the particle size and the residence time. *Fuel Process Technol.* 91, 681-692.
15. Hyland, C., Sarmah, A.K., 2014. Chapter 25 - Advances and Innovations in Biochar Production and Utilization for Improving Environmental Quality, in Gupta, V.K., Kubicek, M.G.T.P., Xu, J.S. (Eds.), *Bioenergy Research: Advances and Applications*. Elsevier, Amsterdam, pp. 435-446.
16. Jadhav, S.G., Vaidya, P.D., Bhanage, B.M., Joshi, J.B., 2014. Catalytic carbon dioxide hydrogenation to methanol: A review of recent studies. *Chem. Eng. Res. Design*. 92, 2557-2567.
17. James R, A.M., Yuan, W., Boyette, M.D., 2016a. The effect of biomass physical properties on top-lit updraft gasification of woodchips. *Energies*. 9(4), 283-295.
18. James R, A.M., Yuan, W., Boyette, M., Wang, d., Kumar, A., 2016b. Characterization of biochar from rice hulls and woodchips produced in a top-lit updraft biomass gasifier. *Transactions of the ASABE* 59(3): 749-756.
19. Joseph, S., Peacocke, C., Lehmann, J., Munroe, P., 2009. Developing a Biochar classification and test methods, in Lehmann J., Joseph S. (Eds.), *Biochar for*

- Environmental Management: Science and Technology. Earthscan, London, pp. 107-126.
20. Kammen, D.M., Lew, D.J., 2005. Review of technologies for the production and use of charcoal, Renewable and Appropriate Energy Laboratory Report. Available at: http://rael.berkeley.edu/old_drupal/sites/default/files/old-site-files/2005/Kammen-Lew-Charcoal-2005.pdf (accessed: October 7, 2015)
 21. Knoef, H., Ahrenfeldt, J., 2005. Handbook biomass gasification. BTG biomass technology group, The Netherlands.
 22. Lehmann, J., Joseph, S., 2009. Biochar for environmental management: science and technology. Earthscan, London.
 23. Lorenz, K., Lal, R., 2014. Biochar application to soil for climate change mitigation by soil organic carbon sequestration. *J. Plant Nutr. Soil Sci.* 177, 651-670.
 24. Lv, P.M., Xiong, Z. H., Chang, J., Wu, C. Z., Chen, Y., Zhu, J. X., 2004. An experimental study on biomass air–steam gasification in a fluidized bed. *Bioresource Technology.* 95, 95-101.
 25. Lv, P., Yuan, Z., Ma, L., Wu, C., Chen, Y., & Zhu, J., 2007. Hydrogen-rich gas production from biomass air and oxygen/steam gasification in a downdraft gasifier. *Renewable Energy.* 32, 2173-2185.
 26. Ma, Z., Ye, J., Zhao, C., & Zhang, Q., 2015. Gasification of rice husk in a downdraft gasifier: The effect of equivalence ratio on the gasification performance, properties, and utilization analysis of byproducts of char and tar. *Bioresources.* 10, 2888-2902.
 27. Manya J.J. 2012. Pyrolysis for biochar purposes: a review to establish current knowledge gaps and research needs. *Environ Sci. Technol.* 46, 7939-7954.

28. McCord, J., Owens, V., Rials, T., Stokes, B., 2014. Summary Report on the 2012 Sun Grant National Conference: Science for Biomass Feedstock Production and Utilization. *BioEnergy Research*. 7, 765-768.
29. Milne, T.A., Abatzoglou, N., Evans, R.J., 1998. Biomass gasifier" tars": their nature, formation, and conversion. Available at: http://www.ps-survival.com/PS/Gasifiers/Biomass_Gasifier_Tars_Their_Nature_Formation_And_Conversion_1998.pdf (Last accessed: October 7, 2015).
30. Oyedun, A.O., Lam, K.L., Hui, C.W., 2012. Charcoal production via multistage pyrolysis, *Chin. J. Chem. Eng.* 20, 455-460.
31. Panwar, N. L., & Rathore, N. S., 2008. Design and performance evaluation of a 5 kW producer gas stove. *Biomass and Bioenergy*, 32, 1349-1352.
32. Peterson, S.C., Jackson, M.A., 2014. Simplifying pyrolysis: Using gasification to produce corn stover and wheat straw biochar for sorptive and horticultural media. *Industrial Crops and Products*. 53, 228-235.
33. Qian, K., Kumar, A., Patil, K., Bellmer, D., Wang, D., Yuan, W., Huhnke, R.L., 2013. Effects of biomass feedstocks and gasification conditions on the physiochemical properties of char. *Energies*. 6, 3972-3986.
34. Ryu, C., Yang, Y. B., Khor, A., Yates, N. E., Sharifi, V. N., & Swithenbank, J., 2006. Effect of fuel properties on biomass combustion: Part I. Experiments—fuel type, equivalence ratio and particle size. *Fuel*. 85, 1039-1046.
35. Saravanakumar, A., Haridasan, T., Reed, T.B., Bai, R.K., 2007. Experimental investigation and modelling study of long stick wood gasification in a top lit updraft fixed bed gasifier. *Fuel*. 86, 2846-2856.

36. Sparrevik, M., Adam, C., Martinsen, V., Jubaedah, Cornelissen, G., 2015. Emissions of gases and particles from charcoal/biochar production in rural areas using medium-sized traditional and improved “retort” kilns. *Biomass Bioenergy*. 72, 65-73.
37. Tryner, J., Willson, B.D., Marchese, A.J., 2014. The effects of fuel type and stove design on emissions and efficiency of natural-draft semi-gasifier biomass cookstoves. *Energy for Sustainable Development*. 23, 99-109.
38. Tryner, J., Tillotson, J. W., Baumgardner, M. E., Mohr, J. T., DeFoort, M. W., & Marchese, A. J., 2016. The effects of air flow rates, secondary air inlet geometry, fuel type, and operating mode on the performance of gasifier cookstoves. *Environmental Science & Technology*. 50, 9754-9763.
39. Turn, S., Kinoshita, C., Zhang, Z., Ishimura, D., Zhou, J., 1998. An experimental investigation of hydrogen production from biomass gasification. *Int. J. Hydrogen Energy*. 23, 641-648.
40. Weiland, F., Wiinikka, H., Hedman, H., Wennebro, J., Pettersson, E., & Gebart, R., 2015. Influence of process parameters on the performance of an oxygen blown entrained flow biomass gasifier. *Fuel*. 153, 510-519.

Fig. 1. Illustration of the top-lit updraft gasifier and syngas and tar sampling systems.

Fig 2. The pyrolysis front temperature of (A) rice hulls and (B) woodchips; average reaction temperature of (C) rice hulls and (D) woodchips.

Fig. 3. The temperature profile of (A) rice hulls and (B) woodchips showing movement of flame (airflow of 12 lpm); the burning rate of (C) rice hulls and (D) woodchips at the two insulation conditions. TC-1 (thermocouple 1), TC-2 (thermocouple 2).

Fig. 4. The biochar yield (wt% db) of (A) rice hulls and (B) woodchips at the two insulation conditions; tar content in biochar (wt% db) from (C) rice hulls and (D) woodchips. Different letters indicate significant differences by Tukey's HSD test ($\alpha=0.1$).

Fig. 5. Tar content in syngas from (A) rice hulls and (B) woodchips at the two insulation conditions. Different letters indicate significant differences by Tukey's HSD test ($\alpha=0.1$).

Fig. 6. The mass balance of rice hulls gasification (A) without insulation and (B) with insulation; the mass balance of woodchips gasification (C) without insulation and (D) with insulation.

Figure 1

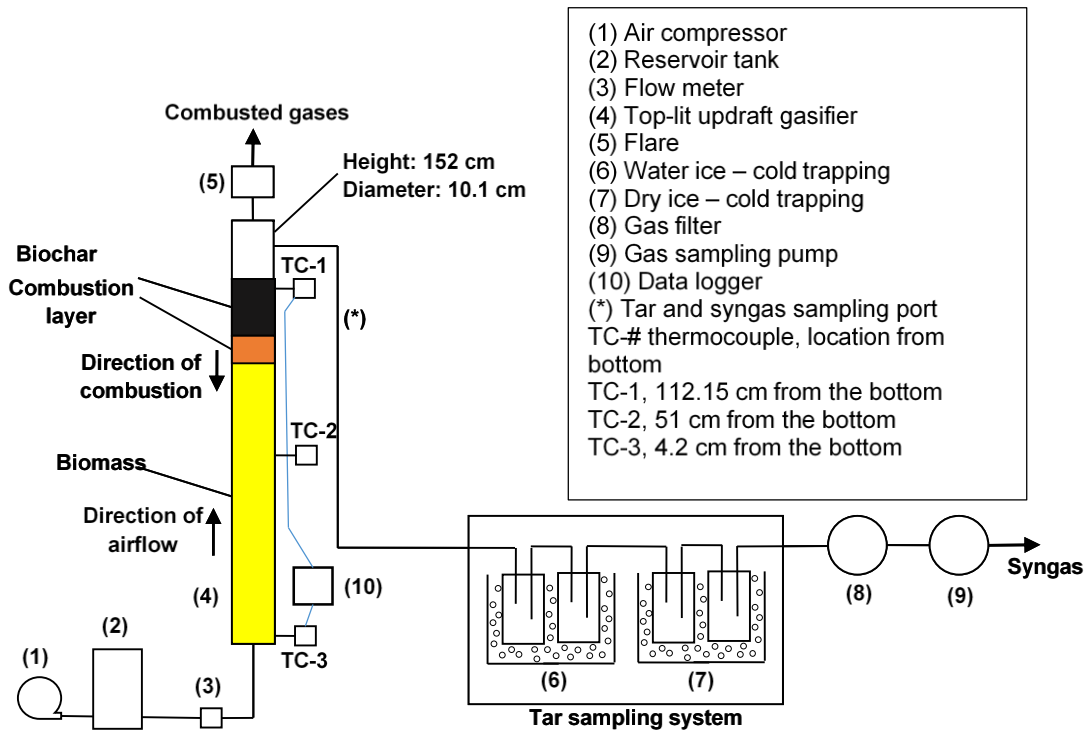


Figure 2

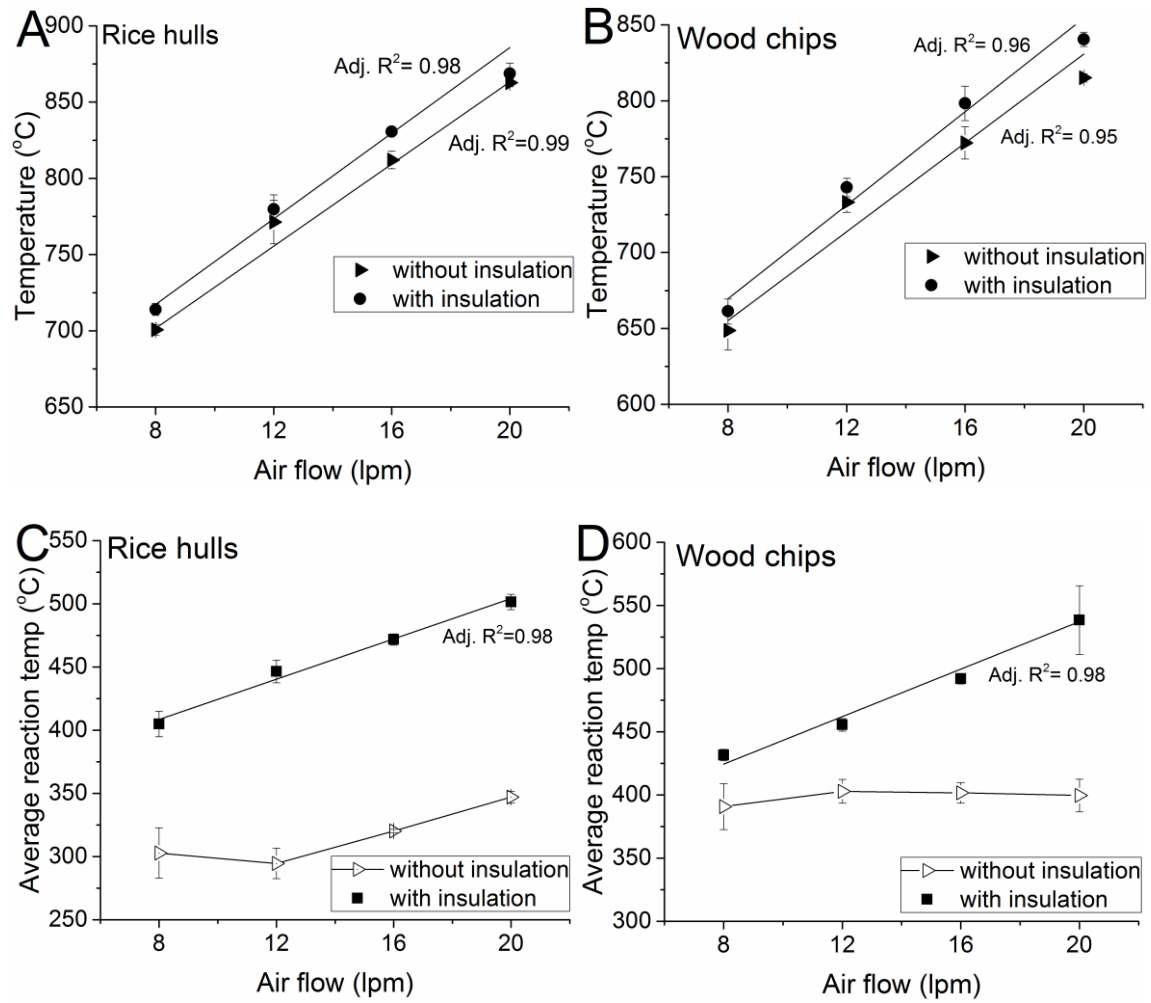


Figure 3

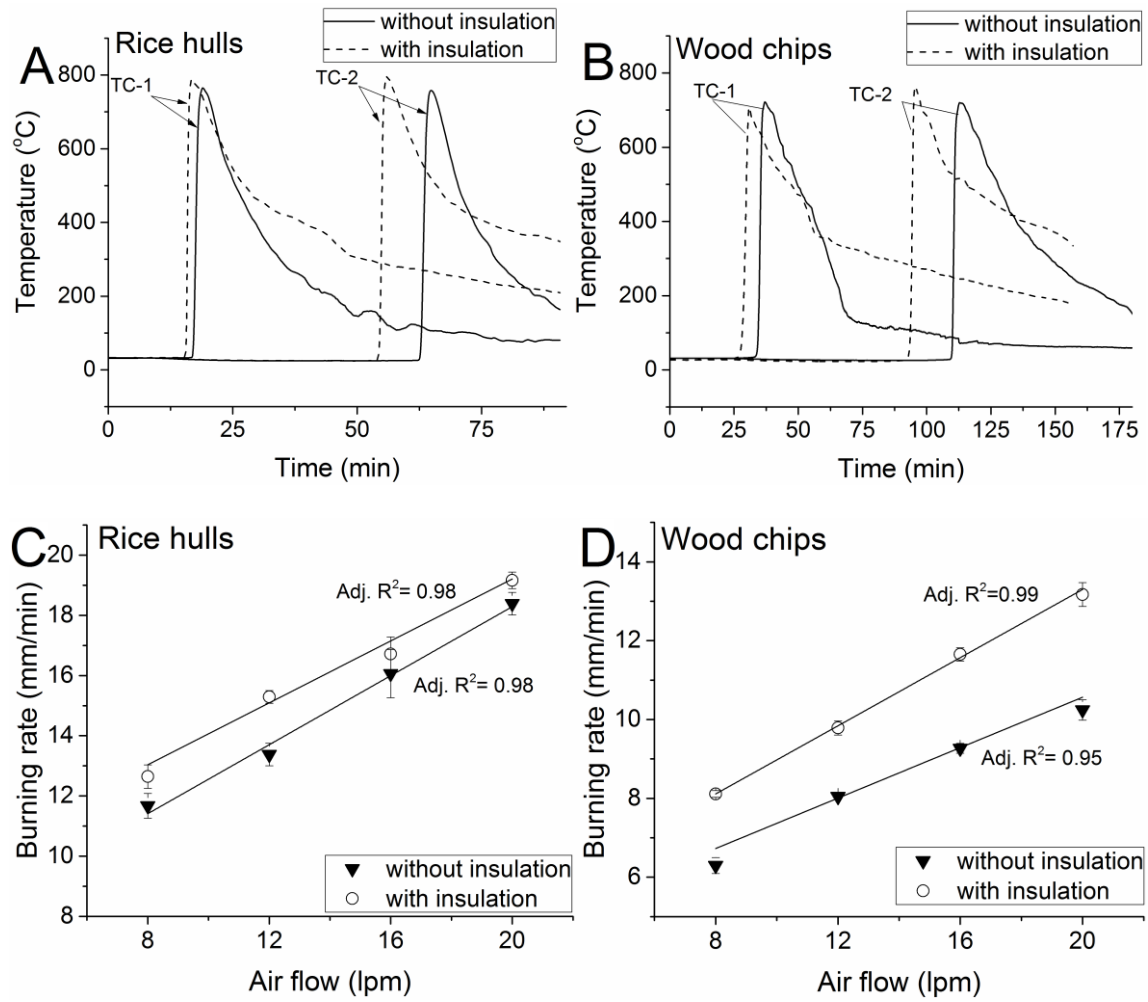


Figure 4

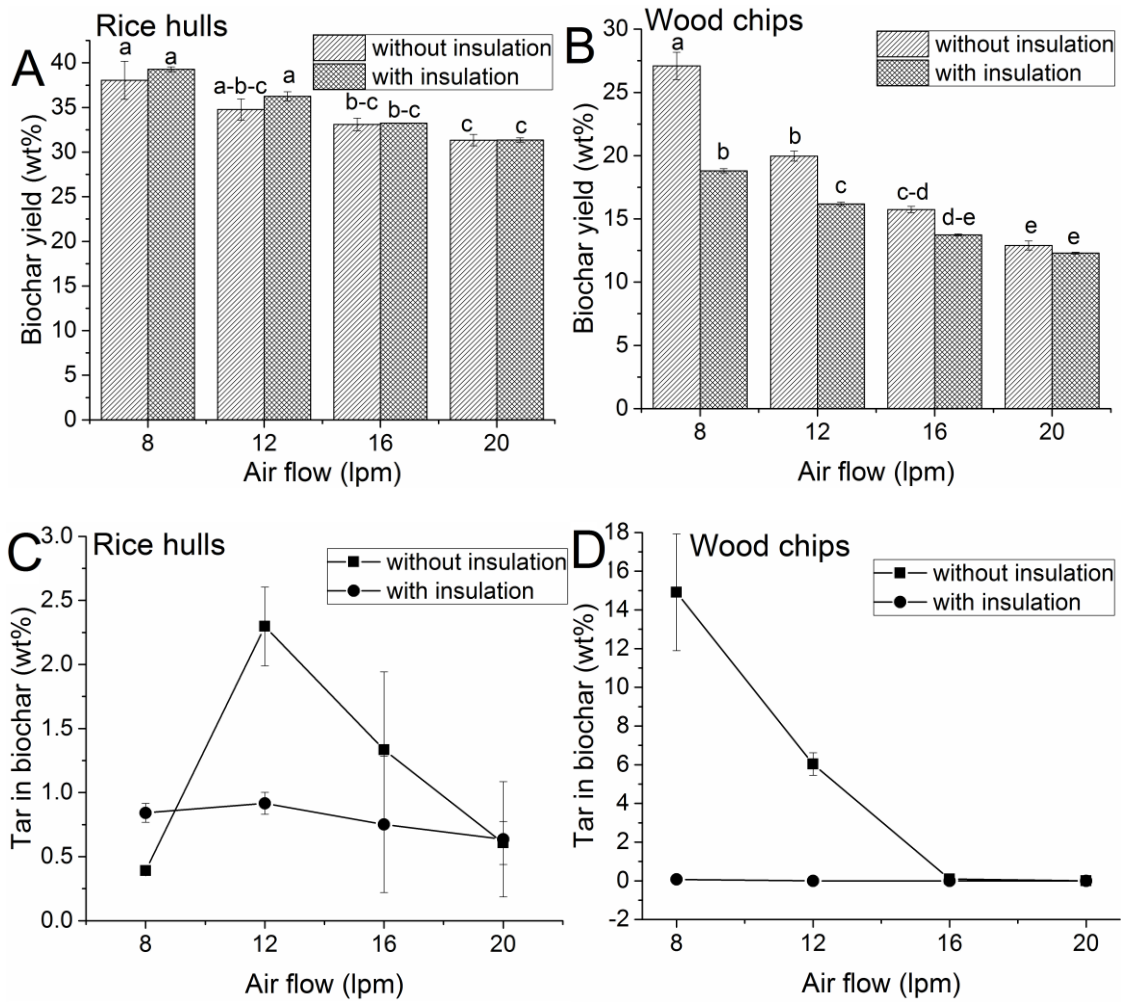


Figure 5

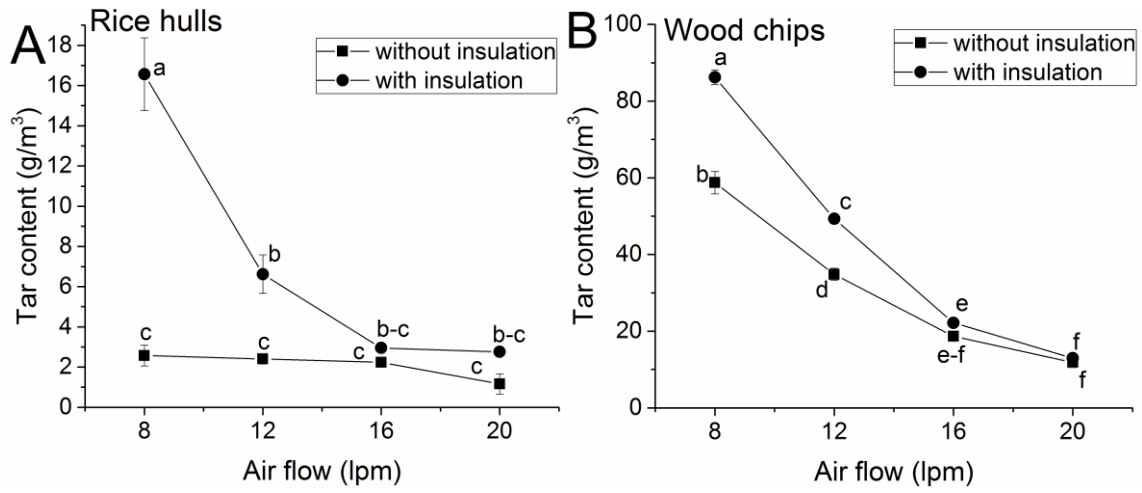


Figure 6

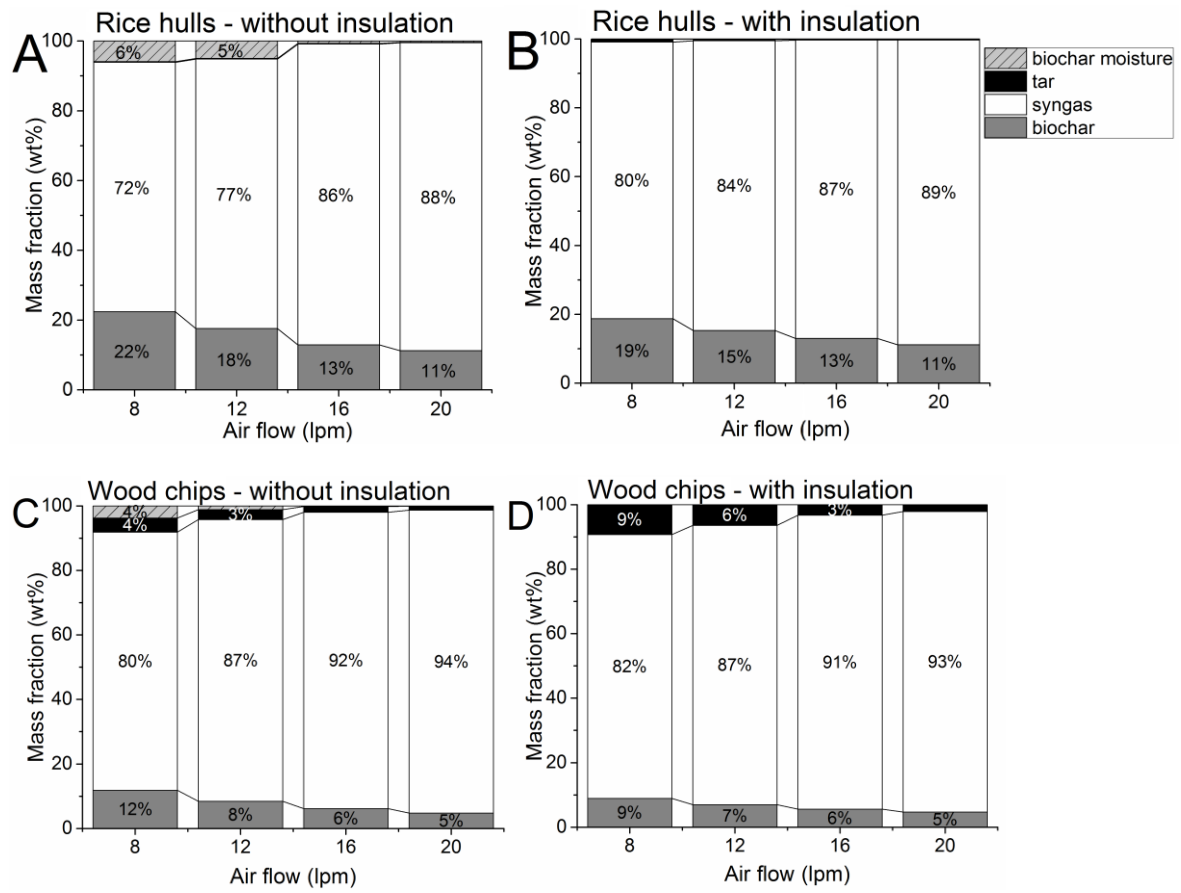


Table 1. Properties of rice hulls and wood chips.

	Biomass	
	Rice hulls	Woodchips
C (%)	36.99	47.90
H (%)	5.14	1.70
N (%)	0.58	0.30
O ^a (%)	56.30	49.90
S (%)	1.0	0.20
Ash (%)	23.78	0.57
Volatile matter (%)	58.17	74.92
Fixed carbon ^a (%)	9.57	16.66
Moisture (%)	8.48	7.85
Bulk density (g/cm ³)	1.27	2.11
Particle size (mm)	X ≤ 2	3 < X ≤ 10

^a calculated by difference

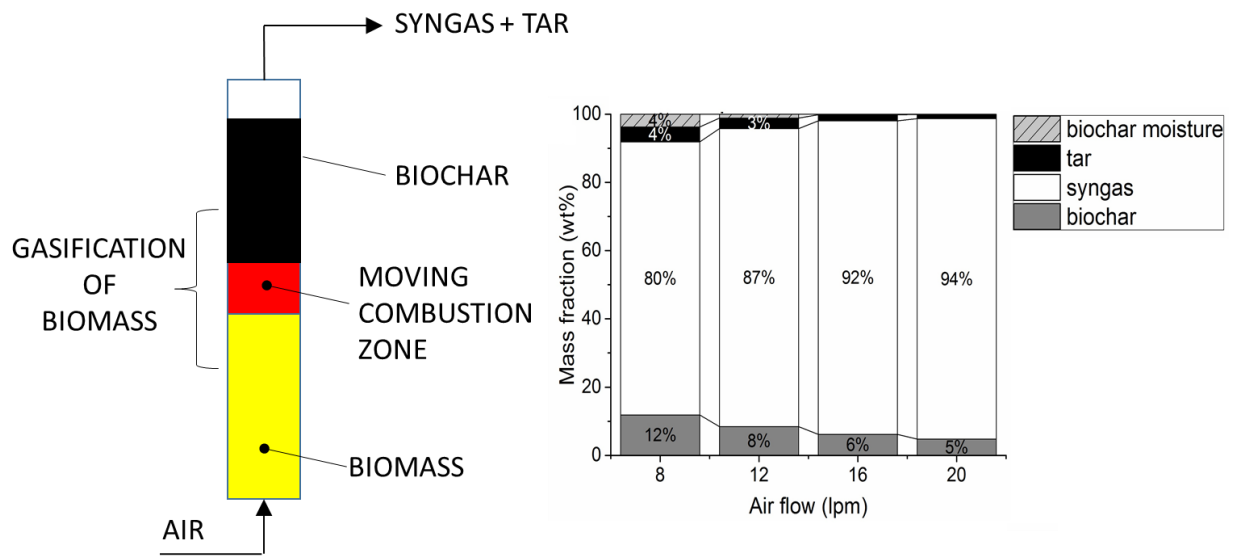
Table 2. Hydrogen and carbon monoxide compositions (v/v %) in syngas.

		without insulation			with insulation		
	Airflow (lpm)	H ₂ (%)	CO (%)	CO ₂ (%)	H ₂ (%)	CO (%)	CO ₂ (%)
Rice Hulls	8	2.34±0.13	13.49±0.31	13.31±0.50	2.83±0.30	14.22±0.56	12.86±0.11
	12	2.68±0.24	12.31±0.50	11.75±0.62	3.69±0.46	15.09±0.73	12.50±0.51
	16	4.02±0.11	15.25±0.16	12.00±0.43	4.26±0.17	15.97±0.06	11.83±0.13
	20	4.23±0.12	14.85±0.41	11.75±0.33	4.44±0.13	15.80±0.21	12.22±0.06
Wood chips	8	2.56±0.33	11.45±0.69	12.78±1.16	3.31±0.21	13.72±0.28	13.36±0.19
	12	5.06±0.14	14.35±0.52	13.68±0.56	4.68±0.17	14.27±0.37	13.35±0.87
	16	5.57±0.16	14.83±0.36	14.22±0.27	5.43±0.07	14.23±0.29	13.27±0.41
	20	5.70±0.54	13.76±0.54	14.02±0.43	6.61±0.38	14.97±0.22	13.48±0.68

Table 3. Effect of biomass type on gasification performance. Different letters among analyses indicate significant differences in the order of a>b>c>d>e.

	Rice hulls				Wood chips			
Airflow (lpm)	8	12	16	20	8	12	16	20
Pyrolysis front temperature (°C)	c	b	a	a	d	c	b	a
Average reaction temperature (°C)	b	ab	ab	ab	ab	ab	ab	a
Burning rate (mm/min)	bc	b	a	a	e	de	cd	c
Biochar yield (wt. %)	a	ab	b	b	c	d	de	e
Tar content in syngas (g/m ³)	cd	d	d	d	a	b	c	cd
Syngas HHV (MJ/m ³)	abc	bc	ab	ab	c	ab	a	a
H ₂ in syngas (v/v %)	e	de	c	cd	e	bc	ab	a
CO in syngas (v/v %)	NS	NS	NS	NS	NS	NS	NS	NS

NS – not significant. HHV – Calculated from H₂, CO and CH₄.



41.